Chemical Science

ROYAL SOCIETY OF CHEMISTRY

EDGE ARTICLE

View Article Online
View Journal | View Issue

Cite this: *Chem. Sci.*, 2020, **11**, 10705

All publication charges for this article have been paid for by the Royal Society of Chemistry

Received 11th May 2020
Accepted 15th June 2020

DOI: 10.1039/d0sc02694h

rsc.li/chemical-science

H/D exchange under mild conditions in arenes and unactivated alkanes with C_6D_6 and D_2O using rigid, electron-rich iridium PCP pincer complexes†

Joel D. Smith,[a] George Durrant,[b] Daniel H. Ess,[b] Benjamin S. Gelfand[a] and Warren E. Piers*[a]

The synthesis and characterization of an iridium polyhydride complex (**Ir-H$_4$**) supported by an electron-rich PCP framework is described. This complex readily loses molecular hydrogen allowing for rapid room temperature hydrogen isotope exchange (HIE) at the hydridic positions and the α-C–H site of the ligand with deuterated solvents such as benzene-d_6, toluene-d_8 and THF-d_8. The removal of 1–2 equivalents of molecular H_2 forms unsaturated iridium carbene trihydride (**Ir-H$_3$**) or monohydride (**Ir-H**) compounds that are able to create further unsaturation by reversibly transferring a hydride to the ligand carbene carbon. These species are highly active hydrogen isotope exchange (HIE) catalysts using C_6D_6 or D_2O as deuterium sources for the deuteration of a variety of substrates. By modifying conditions to influence the **Ir-H$_n$** speciation, deuteration levels can range from near exhaustive to selective only for sterically accessible sites. Preparative level deuterations of select substrates were performed allowing for procurement of >95% deuterated compounds in excellent isolated yields; the catalyst can be regenerated by treatment of residues with H_2 and is still active for further reactions.

Introduction

Metal-catalyzed hydrogen isotope exchange (HIE) is a key fundamental process for preparing isotopically labeled organic compounds necessary for studying reaction mechanisms and biological metabolic processes.[1] Since the seminal work on homogeneous HIE by Garnett and Hodges[2,3] as well as Shilov and co-workers,[4,5] advances in analytical biology and chemistry have created an ever growing demand for deuterium[6] and tritium[7] labeled molecules.[8] Consequently, an important body of research devoted to studying the homogeneously catalyzed exchange of hydrogen and deuterium atoms (H/D exchange) has developed over the last 25 years.[9–12] Pioneering work by the Bergman group on pentamethylcyclopentadienyl supported iridium hydrides demonstrated low temperature C–H activation[13–15] and it was subsequently shown that H/D exchange by cationic iridium complexes[16–18] occurred under relatively mild conditions using C_6D_6 as a deuterium source. Most of these transformations involved selective deuterium incorporation into arene substrates[10,11] with only a handful of catalysts capable of H/D exchange on unactivated alkane substrates under more forcing conditions.[16,17,19–24]

Tridentate "pincer" ligands have played a prominent role in homogeneous catalysis.[25,26] For example, polyhydridic pincer complexes of the late transition metals (particularly Ru and Ir) are known to be exemplary alkane dehydrogenation[27] and CO_2 reduction catalysts,[28,29] but recent work has demonstrated their promise as competent catalysts for promoting homogenous H/D exchange. Leitner, Milstein and co-workers were the first to show that a Ru based PNP polyhydride, **I** Chart 1, could use C_6D_6 or D_2O for arene deuteration at 50 °C.[30,31] Shortly after, Zhou and Hartwig revealed that the aliphatic iridium PCP polyhydride **II** could be used as a pre-catalyst to efficiently perform H/D exchange between olefins and C_6D_6 at room temperature without isomerization.[32] Following these reports, PNP (**III**) and PCP (**IV**) complexes synthesized by Grubbs[33] and Wendt,[34] respectively, were also tested as HIE mediators. The iridium dihydride species **III** was able to selectively deuterate aromatic compounds and silanes, while the cyclohexyl-based PCP complex **IV** was found to successfully deuterate arenes and to a limited extent C_{sp^3}–H sites, albeit at elevated temperatures of 150 °C.

Design elements of the ligands **II**/**IV** and **III** have been incorporated into a family of PCP ligands **V** introduced by our group[35] and also explored by others.[36–39] An attractive feature of these ligands is their ability to assume $PC_{sp^3}P$ or $PC_{carbene}P$ forms by the addition or removal of a hydrogen atom from the

[a]*Department of Chemistry, University of Calgary, 2500 University Drive NW, Calgary, Alberta T2N 1N4, Canada. E-mail: wpiers@ucalgary.ca*

[b]*Department of Chemistry and Biochemistry, Brigham Young University, Provo, Utah 84602, USA*

† Electronic supplementary information (ESI) available: Synthesis, characterization data, experimental and computational details. CCDC 2002787 for **Ir-H$_4$** and 2002788 for **Ir-Ph**. For ESI and crystallographic data in CIF or other electronic format see DOI: 10.1039/d0sc02694h

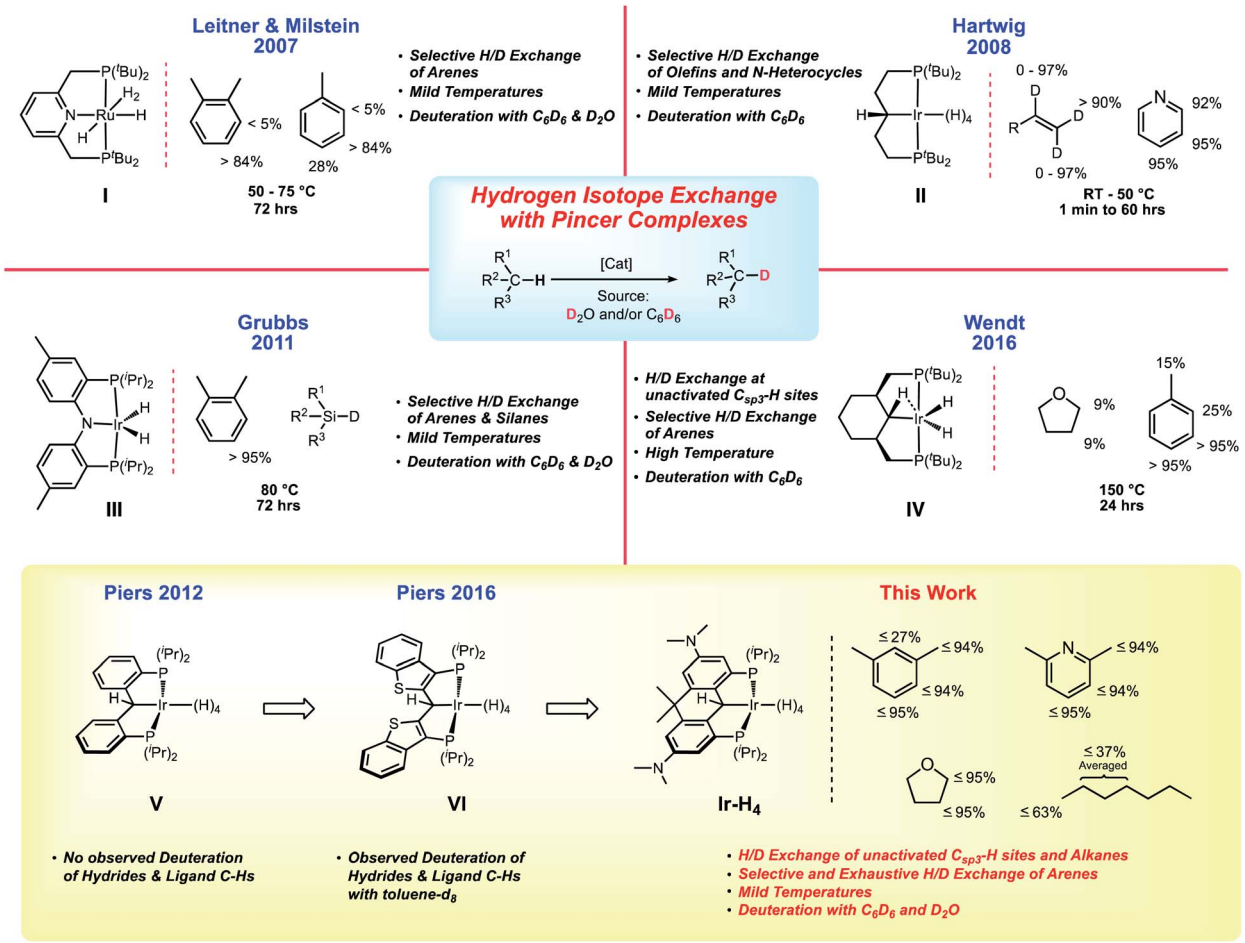

Chart 1 Contextualization of this study.

anchoring carbon of the pincer framework. This has precedence in the ligands **II** and **IV** but in the aryl-linked PCP systems **V** (and the related benzothiophene-based system **VI**[40]) this is potentially more controllable because of the lack of β-hydrogens in the PCP linker framework, and through manipulation of the electronic properties of the ligand *via* substitution on the aryl linkers and/or rigidification of the ligand *via* additional linking of the backbone aryl groups.[41,42] With these two structural levers, a library of PCP ligands has been prepared and a substantial range of ν_{CO} values has been found for $[(PC_{carbene}P)IrCO]^+$ species.[43] We have shown that the rate of addition of N_2O to the C=Ir bond[40] can therefore be tuned substantially.[44] Furthermore, the rigidification of the ligand tends to favor the $PC_{carbene}P$ form of the ligand *vs.* the $PC_{sp^3}P$ form, while also providing greater protection against C–C bond cleavage reactions that destroy the integrity of the ligand in unlinked systems akin to **V**.[45] The ability of the carbon atom in these PCP pincers to engage in ligand cooperativity has been exploited in hydrogen,[35,46] silane[47–49] and other small molecule[40,50–53] activations in various systems. Furthermore, in polyhydridic systems, the dibenzylic hydrogen is actively involved in exchange with the metal hydrides,[34,35] increasing the "hydrogen capacity" of these compounds relative to other (for example PNP) polyhydridic pincer complexes and potentially providing new pathways for catalysis.

In both the parent, unsubstituted, unlinked system **V**,[35] and that incorporating the benzothiophene-based ligand **VI**,[46] the Ir polyhydride is only stable under an atmosphere of dihydrogen but it was observed that slow H/D exchange in the sterically exposed C–H bonds of the ligand aryl backbone occurred in C_6D_6. We hypothesized that a more electron rich system would accelerate this process and indeed, the linked dihydroanthracene PCP ligand framework fitted with electron donating dimethylamino groups *para* to the PCP carbon (bottom of Chart 1) supports a stable, isolable polyhydride species **Ir-H$_4$** (Chart 1). While stable as a solid, this complex readily loses molecular hydrogen in solution to give species that are highly active HIE catalysts at low loadings and under mild conditions. Both C_6D_6 and D_2O can be used as deuterium sources and selectivity can be modulated to some extent by controlling the catalyst speciation.

Results and discussion

Synthesis and characterization of iridium PCP pincer polyhydride Ir-H$_4$

Using methodology established previously,[46,54] the iridium PCP pincer complex **Ir-OH** was prepared by heating the previously

reported **Ir-Cl**[44] to 120 °C in toluene with an excess of CsOH for 24 hours (Scheme 1, red arrows). The resulting brown solution was filtered through Celite® and a brown powder was isolated in 80% yield after removing all volatiles *in vacuo*. The **Ir-OH** complex displays a characteristic –OH triplet ($^3J_{HP}$ = 3.8 Hz) at 3.62 ppm in the ^{1}H NMR spectrum as well as a singlet in the ^{31}P{^{1}H} NMR at 51.9 ppm. The presence of an iridium-carbene moiety was indicated by a triplet signal at 196.0 ppm ($^2J_{CP}$ = 2.2 Hz) in the ^{13}C{^{1}H} NMR spectrum.

Dissolving **Ir-OH** in benzene and exposing it to 4 atm of H_2 gas for 3 hours resulted in a color change from dark reddish-brown to yellow-orange. The ^{31}P{^{1}H} NMR spectrum for the solution exhibited a single peak at 56.5 ppm and upon solvent removal a brown residue was formed. This residue was then stirred in *n*-pentane under 1 atm of H_2 for 20 minutes producing a beige powder, **Ir-H$_4$**, that was isolated in 98% yield following the removal of all volatiles *in vacuo*. Alternatively, we found stirring the precursor **Ir-Cl** with NaOH (10 eq.) under H_2 gas (4 atm) in benzene for 3 hours produced a similar red-orange solution (Scheme 1, blue arrow). Following filtration through a pad of Celite®, the solution was stirred for 20 minutes under H_2 gas. All volatiles were removed *in vacuo* and a beige powder was again isolated in 94% yield. Compared to the parent *ortho*-phenylene **V**[35] (Chart 1) and the benzothiophene-based ligand congener **VI**,[46] which both could not be isolated due to decomposition *via* loss of H_2 under vacuum, complex **Ir-H$_4$** is remarkably stable as a solid and can be stored indefinitely at room temperature under an inert atmosphere. Furthermore, it can be interrogated *via* NMR spectroscopy in cyclohexane-d_{12} or methylcyclohexane-d_{14} under argon, whereas the others (**V** and **VI**) must be kept under an atmosphere of H_2 in order to avoid decomposition. The ^{1}H NMR spectrum for **Ir-H$_4$** in cyclohexane-d_{12} displays a single triplet (average J_{HP} = 10.2 Hz) resonance at −10.32 ppm and a singlet at 5.52 ppm, integration indicating the presence four rapidly exchanging hydridric nuclei and one α-C(H)–Ir proton, respectively. Moreover, the ligand resonances in the spectrum clearly point to C_s symmetry with 12 equivalent dimethyl amino protons represented by a singlet at 2.85 ppm and two signals at 1.23 ppm and 1.84 ppm for the inequivalent

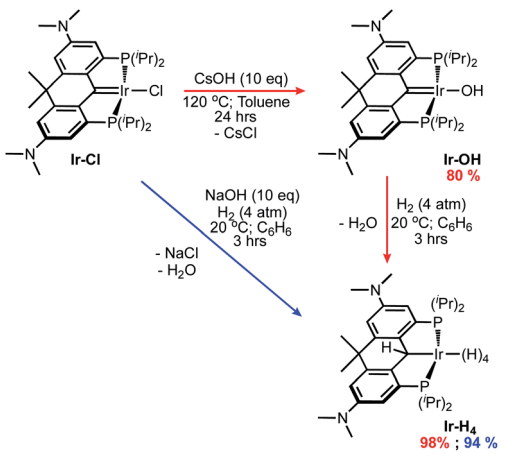

Scheme 1 Synthetic routes to iridium PCP polyhydride **Ir-H$_4$**.

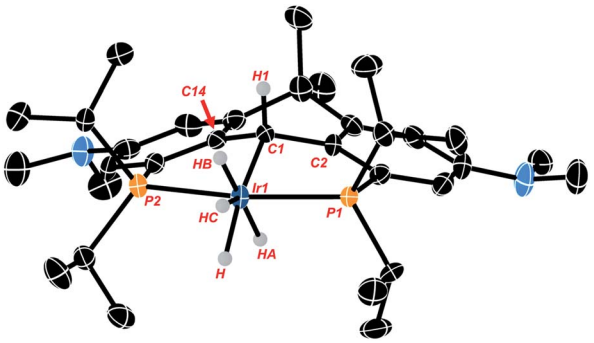

Fig. 1 Thermal ellipsoid diagram of **Ir-H$_4$** (ellipsoids drawn to 50% probability; all hydrogen atoms except H, H1, HA, HB and HC have been omitted for clarity). Selected metrical data for **Ir-H$_4$**: bond distances (Å); Ir1–C1, 2.186(5); Ir1–P1, 2.2703(16); Ir1–P2, 2.2786(16), C1–C2, 1.496(8); C1–C14 1.519(8). Bond angles (°); P1–Ir1–P2, 163.45(5); Ir1–C1–C2, 112.9(4); Ir1–C1–C14, 112.0(4); C2–C1–C14, 110.2(5).

–CH_3 groups attached to the carbon backbone linker. The ^{13}C{^{1}H} NMR also corroborates the formation of **Ir-H$_4$** showing the loss of the carbene triplet associated with the **Ir-Cl** and **Ir-OH** complexes and the presence of a signal at 21.0 ppm coupling to the α-C–H proton at 5.52 ppm in the ^{1}H–^{13}C HSQC spectrum.

Crystals of the compound were obtained by slowly cooling a supersaturated solution of **Ir-H$_4$** in isopropanol from 50 °C to 20 °C and crystallographic analysis corroborates the solution data described above. The hydrogen atoms associated with the metal center were located from the Fourier map but low accuracy in **Ir-H** and H–H distances preclude conclusions concerning their arrangement as hydride or dihydrogen ligands. The data show the anchoring α-carbon (C1 in Fig. 1) is pyramidalized (the sum of the angles about C1 is 335.2(8)°), and the central 6 membered ring containing this α-carbon has also adopted a "boat"-like conformation. The sp^3 hybridization of the α-carbon is also indicated by the central Ir1–C1 bond length of 2.184(5) Å which is similar to other sp^3 hybridized Ir–C bonds we have observed with these NR_2 substituted ligand frameworks[44,45] and lengthened significantly from the values of ≈1.93 Å seen in $PC_{carbene}P$ complexes of this ligand.[44]

Given the lack of crystallographic data concerning the iridium hydrides in **Ir-H$_4$**, we turned to criteria developed by Halpern and co-workers[55] to shed some light on what form dominates the speciation of **Ir-H$_4$** in solution. While it is typically difficult to unambiguously categorize the hydride bonding mode for these complexes, we were able to rule out the possibility that **Ir-H$_4$** is a "non-classical" Ir(I) bis-dihydrogen species (Scheme 2). The T_1 (min) relaxation for the hydridic nuclei of **Ir-H$_4$** in methylcyclohexane-d_{14} (Fig. S1†) was found to be 186 ms at 600 MHz (10 °C ± 0.5 °C), approximately 155 ms when adjusting to a 500 MHz field strength. These values are comparable to those obtained for other PCP pincer polyhydride complexes reported by Heinekey,[56] Wendt[34] and us;[35] a collection of comparative data is given in Table S1.† These data point to an equilibrating mixture of a "classical" Ir(V) tetrahydride and the "intermediate" Ir(III) dihydrogen–dihydride isomers shown

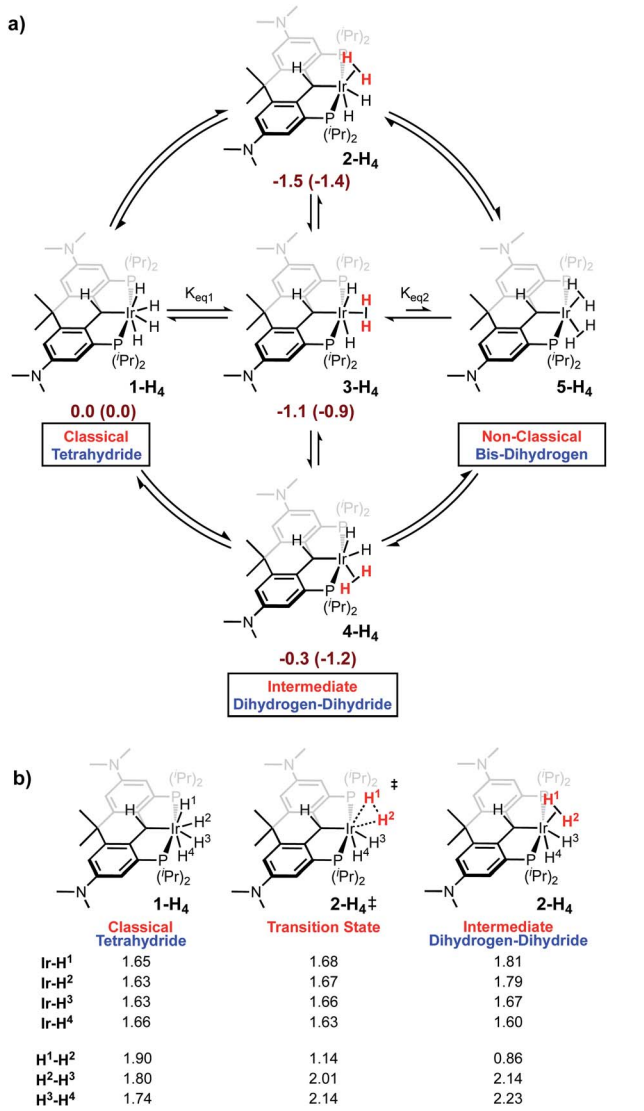

Scheme 2 (a) Outline of isomerism in **Ir-H$_4$** with benzene-solvated enthalpies (Gibbs energies) in kcal mol^{-1} (b) **Ir-H** and H–H distances (Å) found in M06 DFT structures.

in Scheme 2. The experimental T_1 of 155 ms is somewhat lower than the calculated T_1 value of 203 ms calculated from the parameters obtained from the M06 density functional theory (DFT) optimized structure of **Ir-H$_4$**, suggesting a significant contribution from any or all of the dihydrogen–dihydride isomers, which also can be optimized using DFT and give rise to T_1 values of ≈15 ms using the Halpern methodologies. Significantly, the non-classical bis-dihydrogen structure could not be optimized by DFT, suggesting that this formally Ir(I) isomer is not favored with this electron rich pincer ligand and does not contribute to the speciation of **Ir-H$_4$** in solution.

Another key metric in this family of compounds is the averaged J_{H-D} coupling constant in the **Ir-HD$_3$** isotopologue. For **Ir-H$_4$**, this species is trivially prepared by dissolving **Ir-H$_4$** in C_6D_6 and stirring for 15 minutes at room temperature (*vide infra*), removing the solvent and redissolving the sample in methylcyclohexane-d_{14}. All four iridium hydrides and the benzylic position on the ligand are rapidly deuterated under these conditions, but by halting before full deuteration, the residual hydride resonance in methylcyclohexane-d_{14} at −10.25 ppm displays a resolved seven line pattern with an average observed J_{H-D} of 3.1 ± 0.1 Hz when collected at 50 °C (Fig. S2†). This coupling correlates to an approximated average H–H atomic distance of 1.02–1.25 Å (Table S1†),[56] and is consistent with equilibrating classical tetrahydride (H–H > 1.2 Å) and intermediate dihydrogen (H–H ≈ 1.0–1.2 Å) dihydride structures (Table S1†)[57–59] as depicted in Scheme 2. Unlike the related system based on **IV**, attempts to freeze out the exchange between the isomers of the latter and/or the equilibrium between the two *via* variable temperature $^1H\{^{31}P\}$ NMR spectroscopy on **Ir-H$_4$** in methylcyclohexane-d_{14} showed no decoalescence of the hydride resonance to temperatures as low as −110 °C (Fig. S3†). This indicates a lower energetic barrier for hydride exchange than the estimated 8.7 kcal mol^{-1} at −70 °C reported by Wendt *et al.* in the system **IV**.[34] Indeed, M06 DFT calculations indicate the potential energy surface for postulated tetrahydride and dihydrogen–dihydride complexes is relatively flat with an energy range of <2 kcal mol^{-1} between these four structures (Scheme 2). For the full covalent **Ir-H** bonds, the distances are ∼1.6 Å. In the dihydrogen–dihydride structures, the dihydrogen distances are ∼0.85 Å, which are only slightly stretched compared to free H_2.[59] The barriers are <12 kcal mol^{-1} for conversion between tetrahydride and dihydrogen–dihydride complexes. The transition-state distances for the forming H–H bonds are ∼1.1 Å. Overall, these DFT thermodynamic and kinetic estimates suggest that all intermediate and classical structures are accessible in solution and the spectroscopically observed complex lies within the dihydrogen–dihydride tetrahydride continuum. While the benzylic hydrogen on the C_{sp^3} carbon of the ligand certainly exchanges with the four iridium hydrogens rapidly on the chemical timescale, the two peaks only undergo slight broadening at temperatures below which loss of H_2 and conversion to other species ensues (*vide infra*). Line shape analysis to probe the barrier was not possible with the spectral data available in this system, unlike that of **IV**.[34]

Solution behavior of Ir-H$_4$

While **Ir-H$_4$** is quite stable in the solid state, evidence exists for reversible loss of H_2 in solution (Scheme 3). When dilute solutions in benzene were exposed to vacuum, the pale-yellow color darkened slowly to a maroon-tinged hue. Readmission of H_2 gas to the vessel gave back the yellow solution; monitoring this transformation by NMR spectroscopy indicated that the maroon solution was essentially spectroscopically identical to the yellow solutions of **Ir-H$_4$**. However, when heating solutions of **Ir-H$_4$** to 80 °C under a static vacuum and monitoring by NMR spectroscopy, other resonances became apparent. In the ^1H NMR spectrum, a new resonance at 2.71 ppm in the NMe_2 region and a faint peak at −10.30 ppm were observed in about a 12 : 3 ratio. In the $^{31}P\{^1H\}$ NMR spectrum, resonance at 66.4 ppm grew in relative to that of **Ir-H$_4$** at 56.5 ppm (Scheme 3 and Fig. S4 and S5†). Cooling the sample resulted in loss of this

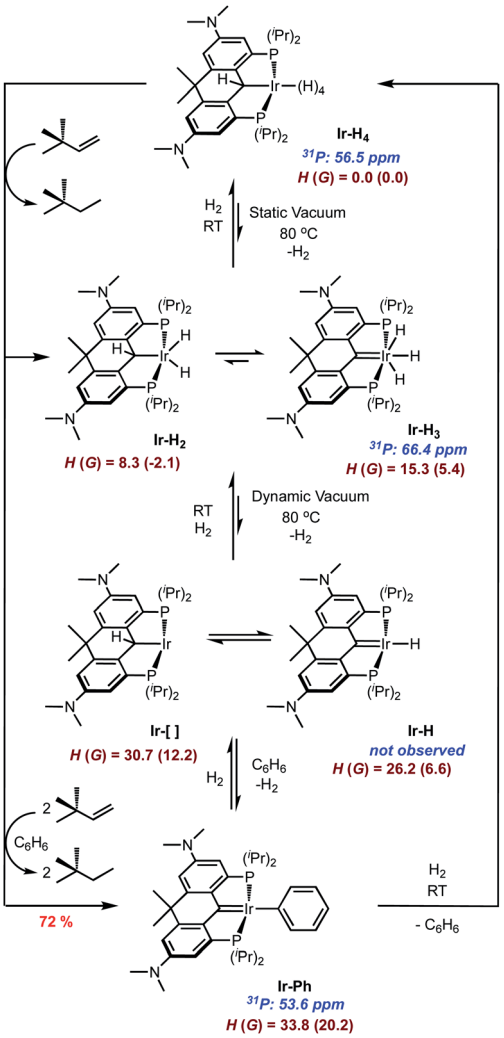

Scheme 3 Solution chemistry of Ir-H_4. Energy units in dark red are kcal mol^{-1}.

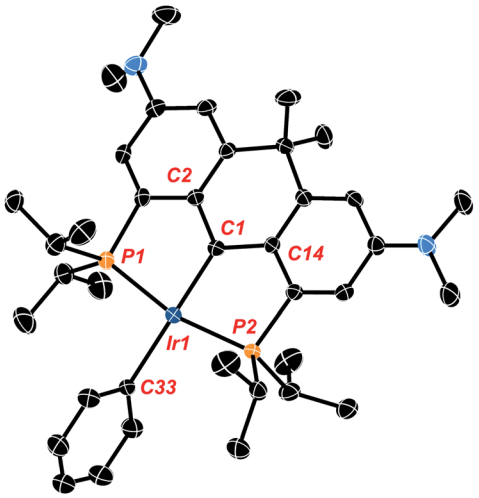

Fig. 2 Synthesis and thermal ellipsoid diagram of **Ir-Ph** (ellipsoids drawn to 50% probability; hydrogen atoms have been omitted for clarity). Selected metrical data for **Ir-Ph**: bond distances (Å): Ir1–C1, 1.965 (4); Ir–C33, 2.118(4); Ir1–P1, 2.2581(13); Ir1–P2, 2.2671(17), C1–C2, 1.467(6); C1–C14 1.469(6). Bond angles (°); P1–Ir1–P2, 166.46(4); C1–Ir1–C33, 179.53(19); P1–Ir1–C1, 83.46(13); P1–Ir1–C33, 96.38(13); Ir1–C1–C2, 122.6(3); Ir1–C1–C14, 122.9(4); C2–C1–C14, 114.5(4).

resonance and a return to solutions that were >98% **Ir-H_4**. We hypothesized that this maroon species was either the $PC_{sp^3}P$ supported Ir(III) dihydride **Ir-H_2** or the $PC_{carbene}P$ ligated Ir(III) trihydride **Ir-H_3** shown in Scheme 3. These should be distinguishable by the ^{13}C resonance of the PCP ligand, but because it is produced in such small amounts *via* this method, we sought ways to prepare or at least enrich the speciation of this compound in order to obtain more concentrated samples.

Heating **Ir-H_4** in benzene under *dynamic* vacuum did lead to a much darker colored solution, but the $^{31}P\{^1H\}$ NMR spectra indicated that a third species with a resonance at 53.6 ppm was dominant in these samples. Separate synthesis, NMR spectroscopy and X-ray crystallography confirmed this product to be the $PC_{carbene}P$ Ir(I) phenyl complex **Ir-Ph** (Scheme 3). In attempts to generate **Ir-H_2**/**Ir-H_3** by treating **Ir-H_4** with the dehydrogenation agent *tert*-butyl ethylene, varying mixtures of the three components were obtained depending on the equivalency of olefin employed; when >3 equivalents were used, **Ir-Ph** was cleanly produced and isolated as a green solid in 72% yield. The $^{13}C\{^1H\}$ NMR spectrum of **Ir-Ph** in benzene-d_6 shows a distinct carbene triplet at 221.1 ppm (J_{CP} = 4.2 Hz) while the ^1H NMR spectrum shows three separate aryl proton signals for the new phenyl group as well as characteristic ligand resonances. Crystallographic data (Fig. 2) show a central Ir1–C1 distance of 1.965(4) Å. This is shorter than that found in **Ir-H_4** and indicative of an iridium carbene bond similar to analogous structures.[35,40,43–45] Accordingly, unlike the boat-like shape found in the **Ir-H_4** the central 6-membered ring of the ligand framework in **Ir-Ph** adopts a planar conformation, as a result of the sp^2 hybridization found at the carbene center. The rigidity of the ligand employed here stabilizes this phenyl complex with respect to the intriguing C–C bond formation reaction observed by Wendt in a the more flexible **IV**.[60]

Taken together, the above observations suggest that **Ir-H_4** rather easily loses one equivalent of H_2, even thermally, to give **Ir-H_2**/**Ir-H_3**, but when exposed to vacuum and heat, a second equivalent of H_2 is eliminated to form the (unobserved) compounds **Ir-[]**/**Ir-H** depicted in Scheme 3. Consistent with the relative ease for H_2 loss, the DFT calculated energy of **Ir-H_3** is only endergonic by ~5 kcal mol^{-1} relative to **Ir-H_4**. Calculations suggest that formation of the dihydrogen–dihydride complex and dihydrogen dissociation is required before 1,2-hydrogen shift from the ligand to Ir to form **Ir-H_3**, which only requires a barrier of ~15 kcal mol^{-1}. The **Ir-H**/**Ir-[]** structures are calculated to be 6.6 and 12.2 endergonic relative to **Ir-H_4**. Overall, the thermodynamic and kinetic DFT calculations suggest that **Ir-H_3**, **Ir-H_2**, **Ir-H**, and **Ir-[]** structures are all viable. These compounds rapidly C–H activate benzene and, after elimination of another equivalent of H_2, **Ir-Ph** is produced; this compound rapidly converts back to **Ir-H_4** upon treatment with H_2, with loss of C_6H_6. The speciation of the **Ir-H_2**/**Ir-H_3** manifold was solidified as being mainly **Ir-H_3** by mixing isolated **Ir-H_4** and **Ir-Ph** in

a ≈2 : 3 ratio in benzene; this experiment resulted in an equilibrium mixture of these two compounds along with about 40% **Ir-H$_3$** which allowed us to acquire meaningful ^{1}H and ^{13}C NMR data on the latter. Both are consistent with C_{2v} symmetry and the presence of a PC$_{carbene}$P ligand. In the ^{1}H NMR spectrum, no resonance in the region between 3 and 6 ppm consistent with the presence of an α-C(H)–Ir proton was observed, while a characteristic resonance at 245.0 ppm in the ^{13}C{^{1}H} NMR spectrum is diagnostic of a carbene carbon. This signal correlated with the triplet integrating to 3 hydrogens at −10.12 ppm in the 2D ^{1}H–^{13}C HMBC spectrum. At room temperature, the single resonance for the three hydrides in **Ir-H$_3$** indicate they are in rapid exchange, presumably *via* a 1,2-hydride shift from the iridium to the carbene carbon, *i.e.*, *via* **Ir-H$_2$**. The apparent thermodynamic preference for **Ir-H$_3$** over **Ir-H$_2$** in this system contrasts with observations reported by Wendt and co-workers,[34,61] but these structures are very close in energy and in rapid exchange. DFT calculations using a variety of functionals (M06, wB97X-D, M11, and others) all indicate that the **Ir-H$_2$** structure is slightly lower in energy than **Ir-H$_3$**, the methodology has limitations for distinguishing these types of isomers accurately.

HIE with iridium polyhydrides Ir-H$_n$

As briefly alluded to above, dissolution of **Ir-H$_4$** into C_6D_6 (and indeed toluene-d_8 or THF-d_8) leads to the rapid deuteration of the α-C(H)–Ir and **Ir-H** positions at 20 °C to form **Ir-D$_4$** (Scheme 4a) and so it had to be characterized in deuterated cyclohexane or methylcyclohexane solvents which do not surrender deuterium at room temperature. Heating **Ir-H$_4$** in C_6D_6 to 65 °C for 24 hours lead to trace deuteration of the ligand NMe$_2$ and iso-propyl methyl groups (Fig. S6†). Given the coordinative saturation of **Ir-H$_4$**, we hypothesized that hydrogen loss to form **Ir-H$_3$** was required to initiate the HIE process. Indeed, mixing **Ir-H$_4$** and **Ir-Ph** as described above to generate solutions enriched in **Ir-H$_3$** leads to much higher deuteration activity. Heating solutions of **Ir-H$_4$**/**Ir-H$_3$**/**Ir-Ph** (3 : 2 : 2) in C_6D_6 to 65 °C for 24 hours gave the three species essentially exhaustively deuterated in the positions shown in Scheme 4b (Fig. S7†). Separate experiments showed that heating pure **Ir-Ph** under these conditions gave only 70% conversion to **Ir-Ph$_{d5}$** after 24 hours and no deuteration of the ligand NMe$_2$ or iso-propyl groups was observed (Fi. S8†), suggesting that **Ir-Ph** is not an effective HIE promoter in this system.

While the ^{i}Pr groups are likely deuterated *via* an intramolecular C–H activation, deuteration of the more remote NMe$_2$ groups suggest that intermolecular catalytic deuteration of other substrates under mild conditions might be possible. We chose *meta*-xylene as a test substrate to evaluate the various iridium species as HIE catalysts due to the sterically varied aryl C–H bonds present, as well as the benzylic sp^3 hybridized C–H bonds. The results of these experiments are summarized in Fig. 3. Solutions containing *meta*-xylene and 1 mol% of either **Ir-H$_4$** (argon, 1 atm), **Ir-H$_4$** (static vacuum), **Ir-Ph** (argon, 1 atm) or **Ir-Ph** activated with D_2 gas (≈1 equivalent) were heated to 50 °C in benzene-d_6 and monitored by ^{1}H NMR spectroscopy. Each

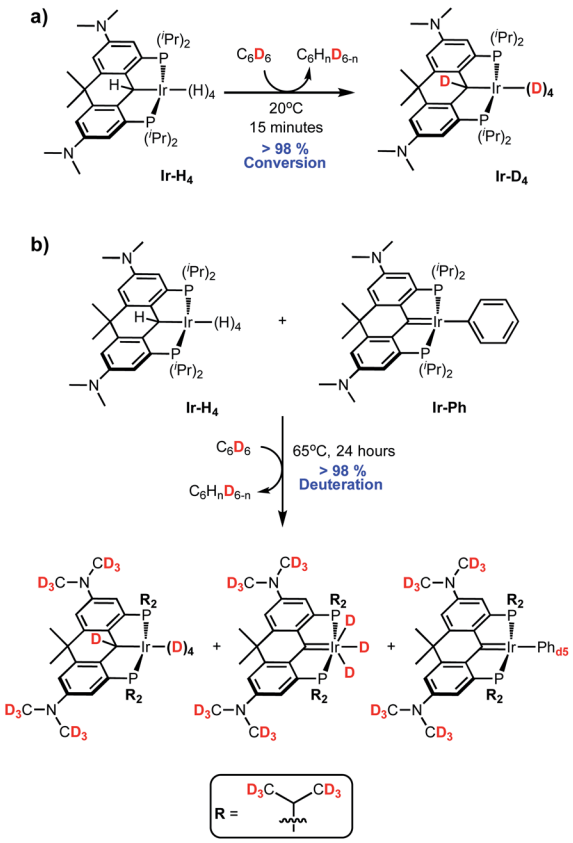

Scheme 4 HIE in Ir-H$_4$.

panel in Fig. 3 indicates the rate of loss of substrate protons as time progresses for a different C–H position in the substrate, as a function of the catalyst precursor employed (colored shapes). Cyclooctane was employed as an internal standard. As can be seen in panel a, none of the catalyst formulations deuterate the sterically encumbered 2 position of *meta*-xylene at 50 °C; the other positions, however, are deuterated to varying degrees. In general, **Ir-H$_4$** under argon and **Ir-Ph** behave similarly for deuteration of the C–H bonds in the benzylic, and aryl 4/5 positions, with moderate activity observed only for the sterically accessible aryl C–H bond in the 5 position. The catalyst systems which would be expected to generate **Ir-[]**/**Ir-H**, (Scheme 3) or **Ir-H$_2$**/**Ir-H$_3$**, namely **Ir-Ph** plus D_2 (blue triangles) or **Ir-H$_4$** under vacuum (green inverted triangles) fared much better, with the former able to almost completely deuterate *meta*-xylene at all three positions under these mild conditions. Notably, when **Ir-H$_4$** is simply exposed to vacuum (green triangles), there is an acceleration in the rate of deuteration consistent with the slow formation of **Ir-H$_3$** through loss of H_2 to the headspace, whereas when the active species is generated through activation of **Ir-Ph** with D_2, a more typical first order time evolution is observed, further implicating **Ir-H$_3$** as the active catalyst or catalyst precursor.

Since it was clear from the above experiments that **Ir-Ph** activated with D_2 gave the most active HIE catalyst, further optimization of conditions for this reaction were undertaken with this as a starting point (Table 1). Entries 1 and 2 reaffirm

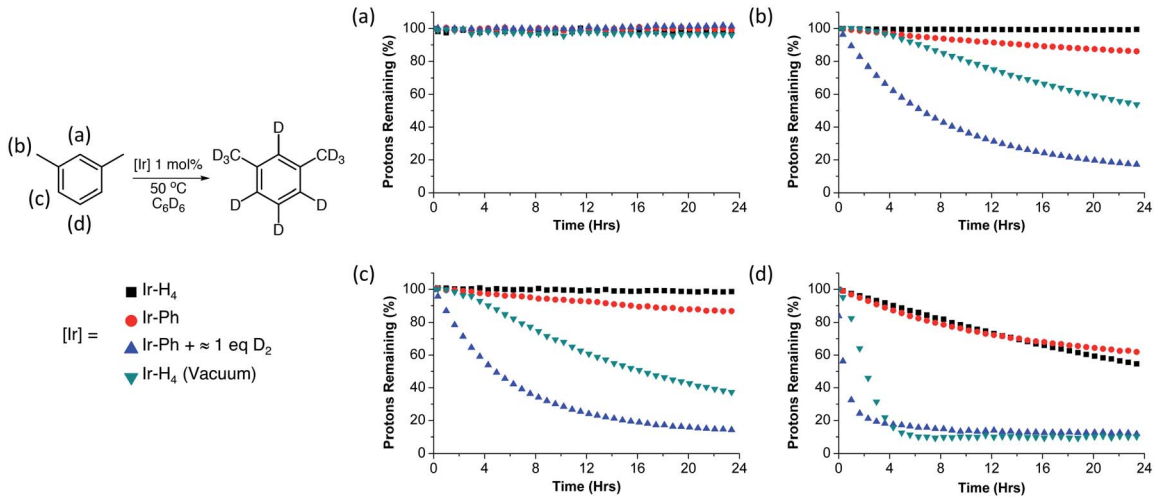

Fig. 3 Reaction profiles of the H/D exchange at the 2 (graph a), benzyl (graph b), 4 and 6 (graph c) and 5 (graph d) position of *m*-xylene (0.38 mmol) in C_6D_6 (0.5 mL) using 1 mol% of either **Ir-H$_4$** (black square), **Ir-H$_4$** placed under static vacuum (green inverted triangle), **Ir-Ph** (red circle) or **Ir-Ph** activated with ≈1 equivalent of D_2 gas (blue triangle). Conversion was measured *via* ^{1}H NMR using cyclooctane as an internal standard.

Table 1 Optimization of conditions for exhaustive deuteration of *meta*-xylene with C_6D_6[a]

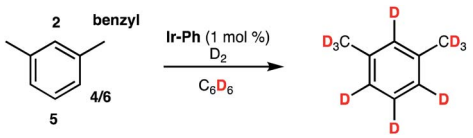

				Position % deuterated (TOF, h^{-1})			
Entry	Temp. (°C)	D_2 (mol%)	Time (h)	Benzyl	2	4/6	5
1	50	No cat.	24	0 (0)	0	0 (0)	0
2	50	0	3.5	3 (1)	0	2 (1)	11 (3)
3	50	1.0	3.5	31 (53)	0	40 (23)	77 (22)
4	50	1.4	3.5	32 (55)	0	41 (23)	81 (23)
5	50	1.8	3.5	26 (45)	0	34 (19)	82 (23)
6	50	3.0	3.5	23 (39)	0	33 (19)	87 (25)
7	50	9.0	3.5	0 (0)	0	0 (0)	8 (2)
8	65	9.0	3.5	0	0	0	20 (6)
9	65	9.0	24	0	0	6 (<1)	70 (3)
10	65	1.4	3.5	69 (118)	4 (1)	77 (44)	88 (25)
11	65	1.4	24	89 (22)	13 (<1)	91 (8)	89 (4)
12[b]	65	1.4	24	94 (24)	27 (1)	95 (8)	95 (4)

[a] Optimization performed with *meta*-xylene (0.38 mmol) and **Ir-Ph** (1 mol%) in C_6D_6 (0.5 mL). D_2 gas was injected into 0.015 M solutions of **Ir-Ph** in C_6D_6 and stirred for 10 minutes prior to its addition to *m*-xylene in C_6D_6 (0.25 mL). Conversion was measured *via* ^{1}H NMR using cyclohexane as an internal standard. [b] Volume of C_6D_6 increased to 1.0 mL.

that a catalyst is required, and that **Ir-Ph** itself is a poor catalyst with low activity. Entries 3–6 show that there is an optimal amount of added D_2 required to activate the catalyst of 1–3 equivalents. With excess D_2 (entry 7), activity drops off markedly, presumably because the iridium speciation is now essentially 100% **Ir-D$_4$**, which (as shown in Fig. 3) is not active under these conditions. Raising the temperature 15 degrees to 65 °C (entries 8–12) leads to greater HIE activity; comparison of entry 4 with entry 10 underscores this observation. Even the difficult 2-position sees some deuteration at this stage. As entries 11 and 12 show, near exhaustive deuteration of the benzylic, 4/6 and 5 positions can be achieved at 65 °C, with 1 mol% of **Ir-Ph** activated with 1.4 equivalents of D_2; entry 12 uses double the amount of C_6D_6 in order to drive the deuteration in these positions to near completion.

In comparison to other PCP (and PNP) pincer catalysts[31–34] for HIE reactions (Chart 1), the iridium systems described here appear to be more active under milder conditions. Furthermore, through manipulation of the speciation of the active **Ir-H$_n$** compounds, the selectivity of deuteration can also be to some extent controlled. Finally, given the stability of these systems to water, D_2O can also be used as a deuterium source rather than

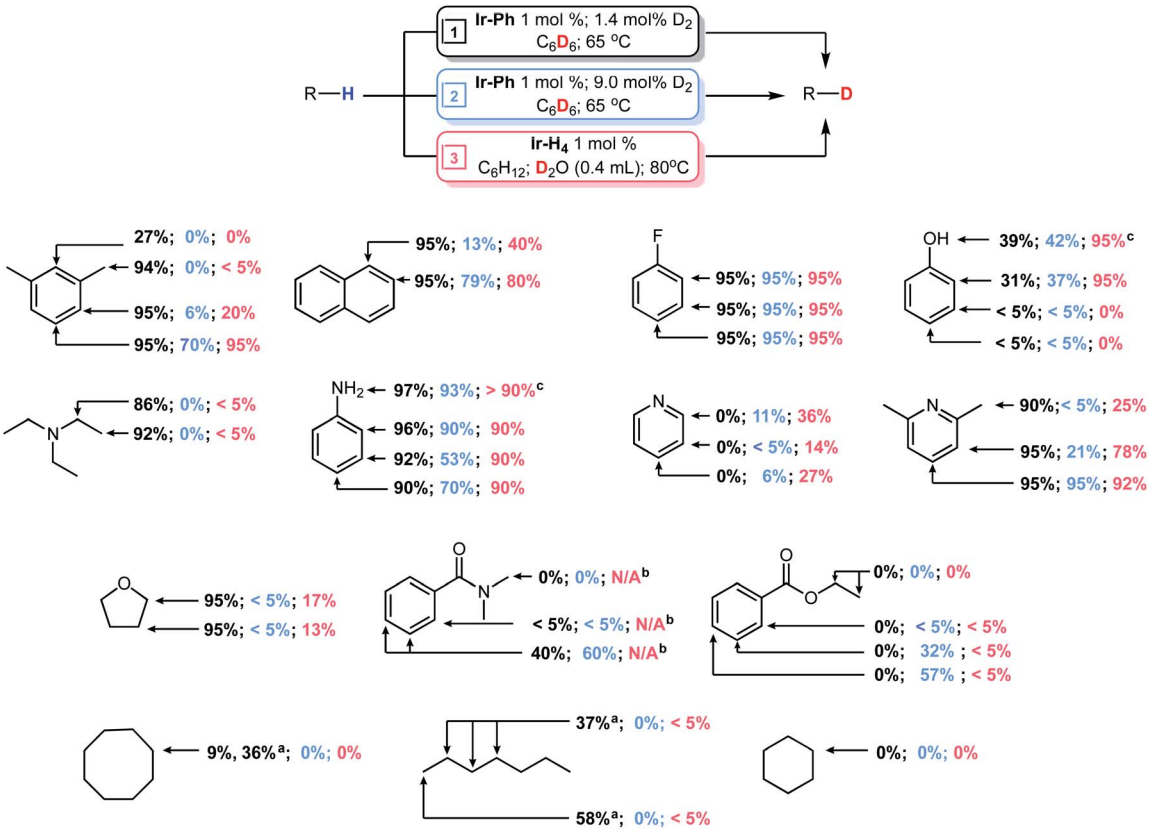

Fig. 4 Distribution of deuterium throughout various substrates following reactions using C_6D_6 or D_2O as a deuterium source. Yields marked black and blue were obtained from reactions with substrates (0.38 mmol) using **Ir-Ph** (1 mol%) activated by 1.4 mol% (black) or 9.0 mol% (blue) of D_2 gas in C_6D_6 (1.0 mL) and heating to 65 °C for 24 hours. Yields marked in red were obtained from reactions with substrates (0.38 mmol) using **Ir-H_4** (1 mol%) in C_6H_{12} (0.750 mL) and heating to 80 °C in the presence of D_2O for 24 hours. Conversion was measured *via* ^{1}H NMR using cyclohexane as an internal standard. For representative spectra for *m*-xylene, see Fig. S22–S24 in the ESI.† [a]Conversion after 5 days at 65 °C. [b]Reaction was not performed due to poor solubility. [c]These positions are deuterated *via* uncatalyzed exchange in D_2O.

C_6D_6. The results of HIE with a number of substrates, under three sets of conditions are summarized in Fig. 4.

Using the optimized conditions of entry 11 in Table 1 developed for *meta*-xylene, HIE for several substrates were examined (Fig. 4, black data). Deuterium incorporation was found to be quite high for several arene based substrates with unhindered C_{sp^2}–H positions in fluorobenzene, naphthalene, aniline and 2,6-lutidine being deuterated almost quantitatively. In the case of naphthalene even the less reactive bay positions were fully deuterated in contrast to **III**[33] and **IV**,[34] which required longer reaction times and higher temperatures to achieve even partial deuteration of these positions in naphthalene. More interestingly, typically less active C_{sp^3}–H positions were significantly deuterated in substrates such as THF, triethylamine, 2,6-lutidine and *meta*-xylene under very mild conditions with no sign of catalyst decomposition. This level of deuteration for the C_{sp^3}–H sites, along with precedents from previous systems,[17,24,62] prompted further investigation into the deuteration of aliphatic hydrocarbons. Despite no detectable H/D exchange occurring between benzene-d_6 and cyclooctane at 50 °C the increased temperature of 65 °C resulted in mild deuteration of 9% after 24 hours which increased to 36% after 5 days. For *n*-heptane, deuteration of the terminal methyl groups was found to be 58% while internal methylene positions were deuterated to 37% after 5 days. The $^{13}C\{^1H\}$ NMR revealed that the majority of deuteration performed on the interior methylene groups occurred the 2 and 6 positions. This is intriguing considering reactivity of cyclopentadienyl Ru complex reported by Nikonov was limited to the terminal methyl C–H sites.[24] Reduced activity was also observed with phenol while catalysis was completely halted in the presence of ethyl benzoate and pyridine. The $^{31}P\{^1H\}$ NMR spectra of these latter reactions showed that complexes **Ir-Ph-d_5**, **Ir-D_3** and **Ir-D_4** were no longer present in solution.

While exhaustive deuteration is desirable in some situations, mild, selective deuteration has some interest for drug discovery and evaluation.[6,8] The data in Table 1 indicates that, under conditions where **Ir-D_4** dominates, deuteration is emphasized at the more sterically accessible sites (see entry 9). We therefore examined HIE with the substrates in Fig. 4 under these conditions (blue data). Using these conditions, good selectivity is possible with compounds containing directing groups and less accessible C_{sp^2}–H sites. While fluorobenzene still showed almost quantitative deuterium incorporation, naphthalene, 2,6-lutidine and *N*,*N*-dimethylbenzamide showed higher levels of deuteration at accessible sites relative to less accessible ones. Catalytic HIE of aniline had a slightly greater preference for

–NH and *ortho*-sites. The increased propensity of the iridium catalyst to bind at the more strongly donating –NH site likely resulted in this mild enhancement. While selectivity was observed in phenol, results were almost identical to the exhaustive conditions with the –OH and *ortho*-positions being deuterated to 42% and 37%, respectively. More surprisingly, deuteration for ethyl benzoate and pyridine became possible. Ethyl benzoate was significantly deuterated at both the *meta*- and *para*-positions while pyridine showed low level deuteration at all sites. For both pyridine and ethyl benzoate, the greater amount of **Ir-D$_4$** may stave off immediate catalyst decomposition by providing increased levels of molecular D_2 present in solution which help prevent these substrates from strongly binding to the iridium center. Under these conditions deuteration at C_{sp^3}–H sites was essentially shut down in all cases.

The use of C_6D_6 as a deuterium source is convenient but in an effort to carry out the reaction with a more economical source of D, we took advantage of the high tolerance of the iridium complexes of this PCP framework towards water and explored the use of D_2O as a deuterating agent for the HIE reaction. Table S2† gives the results of a short optimization study, again using *meta*-xylene as a substrate, and the red data in Fig. 4 shows the results HIE using D_2O with **Ir-H$_4$** under static vacuum as the catalyst precursor. To solubilize the iridium species, reactions were performed in a biphasic mixture of D_2O and cyclohexane.[31,33] For *meta*-xylene, H/D exchange occurred in trace amounts at the benzyl position, 20% at the 4 and 6 positions and quantitatively at the 5 position. Deuteration of the other substrates in Fig. 4 using D_2O gave broadly similar results to those obtained under the "selective" conditions giving rise to the blue data, with a few notable differences. Fluorobenzene was again exhaustively deuterated while naphthalene and 2,6-lutidine had deuterium unevenly distributed throughout the arene systems. Aniline was deuterated almost quantitively in all positions while deuteration in phenol was greatly enhanced to 95%, although limited to the *ortho* and –OH sites. Deuterium levels in pyridine were found to be slightly higher than in the previous attempts but again catalysis was hampered by catalyst degradation (detected *via* $^{31}P\{^1H\}$ NMR). Aliphatic hydrocarbons were found to be mostly unreactive though trace H/D exchange had occurred at the terminal methyl positions of *n*-heptane. Unlike the results produced using **Ir-Ph** and 9 mol% D_2 with benzene-d_6, H/D exchange was found to be possible in both triethylamine and THF, albeit in low levels.

On a preparative scale, these biphasic conditions can be used with neat substrates as summarized in Fig. 5. Both benzene and fluorobenzene (8.3 mmol each) were deuterated at all positions to 90% and 94%, respectively, with D_2O (305 mmol) at 80 °C using 1 mol% of **Ir-H$_4$**. Following extraction of the organic layers and distillation of the liquids, **Ir-H$_4$** was recovered in excess of 90% and deuterated benzene and fluorobenzene were obtained. The experiments were repeated with the recovered **Ir-H$_4$** and deuterium with minimal loss of catalyst performance, as shown in Fig. 5.

Using a slightly modified methodology, both THF and *n*-heptane were partially deuterated and isolated in good yields. **Ir-H$_4$** was not soluble in THF/D_2O mixtures, so a 6 M solution of NaOH in D_2O was employed to render the medium biphasic.[63]

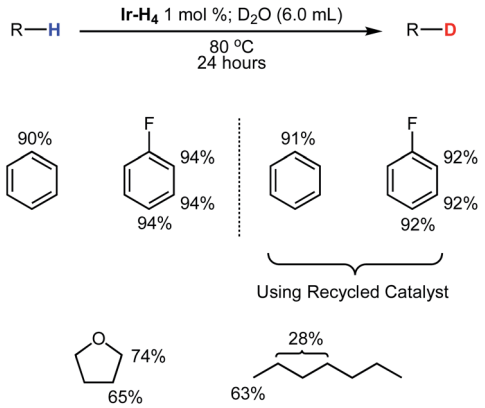

Fig. 5 Distribution of deuterium throughout neat immiscible liquids following reactions using D_2O. Reactions were heated under static vacuum a 80 °C except for THF (100 °C with NaOH (6 M) dissolved in D_2O) and (120 °C).

Heating **Ir-H$_4$** (1 mol%) dissolved in neat THF (8.3 mmol) under static vacuum to 100 °C in the presence of a D_2O with NaOH (6 M) solution resulted in both the 2 and 3 positions were deuterated to 74% and 65%, respectively. Lower temperatures produced significantly lower yields as did performing the reaction under 1 atmosphere of argon. Deuterated THF was isolated *via* distillation and the catalyst was again recovered in 90% yield. NMR analysis of the recovered iridium material in THF revealed the mixture was composed of **Ir-H$_4$**, **Ir-H$_3$** and **Ir-OD** (76%, 3% and 21%, respectively). All material was easily converted back to **Ir-H$_4$** by placing the solution under 4 atmospheres of H_2 gas. In order to partially deuterate *n*-heptane slightly higher temperature (120 °C) was required. After 24 hours the material was isolated and NMR analysis revealed *n*-heptane had been substantially deuterated to 63% at the terminal methyl positions and 28% among all methylene positions.

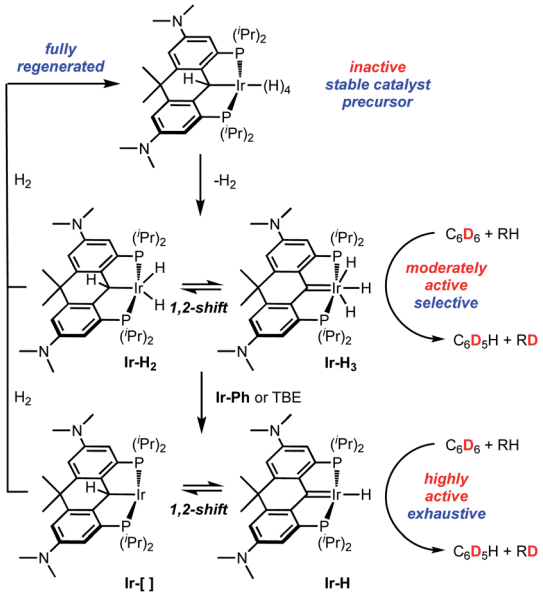

Scheme 5 Summary of ligand design features and their implications for HIE activity in Ir-H$_4$.

Conclusions

Since our initial report in 2012 (ref. 35) on iridium complexes of the $PC_{carbene}P$ framework, buttressed by robust aryl groups linking the arms of the pincer to the central carbene, the ligand design has evolved[40,43,44] into the rigid, planar and highly electron-donating ligand employed here to prepare and isolate **Ir-H$_4$**. Three features of this advanced ligand design make it a highly effective HIE catalyst system (Scheme 5). The electron richness of the ligand allows for the stabilization of the **Ir-H$_4$** form of the catalyst such that it is isolable, storable, and able to fully regenerate if the system is exposed to excess dihydrogen. However, loss of one equivalent of H_2 is facile, allowing for access to the **Ir-H$_2$**/**Ir-H$_3$** manifold, which is moderately active as an HIE catalyst and able to effect selective deuteration of sterically accessible positions on some substrates. We propose that further removal of H_2, formally speaking, allows access to an even more active **Ir-[]**/**Ir-H** catalyst; this species, while not observed experimentally, is implied by the stoichiometry of the reactions that lead to its generation. This species is highly effective at activating a wide variety C–H and C–D bonds *via* oxidative addition, including bonds normally reticent towards activation. While highly reactive, this species is robust under HIE conditions by virtue of the electron richness of the ligand.

A second useful feature in this context, is the ability of these compounds to cooperatively move hydrogen atoms from metal to pincer carbene *via* a low barrier 1,2-shift. This increases their hydrogen capacity in each HIE active manifold while also providing a mechanism for opening coordination space for bond-activating interaction with C_6D_6/D_2O and substrate as is necessary for HIE. This also provides a low barrier path for the H/D scrambling that must occur in order to drive HIE reactions to completion. Finally, the third positive attribute is the rigidity of the ligand framework, as imposed by the aryl groups in the backbone and more crucially the linking Me_2C group. This design element imparts thermal stability by avoiding undesirable catalyst deactivation pathways available to the unlinked variants.[45] Furthermore, this rigidification also makes the 1,2-shift alluded to above more facile by discouraging pyramidalization of the pincer ligand anchoring carbon atom. This has the effect of "flattening the curve" on the energy surface joining the $PC_{sp^3}P$ (as in **Ir-H$_2$** and **Ir-[]**) and $PC_{carbene}P$ (*e.g.* **Ir-H$_3$** and **Ir-H**) forms of the active species by making the C–H bond in the $PC_{sp^3}P$ form weaker and rendering the overall HIE process more efficient. Thus, through advanced ligand design, we have developed a robust, recyclable catalyst for the selective or near exhaustive deuteration of a number of substrates, including on a preparative scale, under mild conditions and using C_6D_6 or D_2O as a deuterium source.

Experimental section

General considerations

All compounds were stored, handled and manipulated, unless otherwise stated, using standard techniques in a VAC glovebox or on a double manifold high vacuum line under an atmosphere of argon purified *via* passage through an OxisorBW scrubber (Model 641-02 Matheson Gas Products). An M-Braun solvent purification system was used to dry *n*-pentane which was subsequently stored over sodium/benzophenone ketal in a 500 mL thick-walled glass pressure flask. Benzene, benzene-d_6, toluene, toluene-d_8, THF-d_8 and cyclohexane were dried over sodium/benzophenone ketal and stored under vacuum in a 100 mL thick-walled glass pressure flask. All dried solvents were degassed and vacuum distilled prior to use. Triethylamine, aniline, pyridine and 2,6-lutidine were dried over CaH_2 and distilled prior to use. Fluorobenzene and ethyl benzoate were dried over 3 Å molecular sieves and filtered off. Methylcyclohexane-d_{14}, cyclohexane-d_{12}, cyclooctane, and *n*-heptane were purchased from Sigma-Aldrich and degassed *via* freeze–pump–thaw prior to use. Phenol, *N*,*N*-dimethylbenzamide and naphthalene were placed under 1 atmosphere of argon prior to use. H_2 (99.5%) and D_2 (99.98%) were purchased from Praxair and used without further purification. Iridium(III) chloride hydrate was purchased from Pressure Chemicals Inc. and used as received. $[Ir(COE)_2Cl]_2$ and **Ir-Cl** were prepared as previously reported.[44,64] ^{1}H and $^{13}C\{^1H\}$ NMR chemical shifts were referenced to residual solvent protons and naturally abundant ^{13}C resonances for all deuterated solvents.[65] Chemical shift assignments are based on ^{1}H, $^{31}P\{^1H\}$, $^{13}C\{^1H\}$, ^{1}H–^{1}H–COSY, ^{1}H–^{13}C–HSQC and ^{1}H–^{13}C HMBC NMR experiments performed on Bruker Ultrashield 400, Ascend-500, or Avance-600 MHz spectrometers using TopSpin *version* 3.2 software. X-ray crystallographic analyses were performed on a Nonius system equipped with a Bruker Apex-II CCD using samples coated in Paratone 8277 oil (Exxon) and mounted on a glass fibre. Elemental analyses were performed by staff of the Instrumentation Facility in the Department of Chemistry, University of Calgary.

Synthesis of Ir-OH

To a 100 mL thick walled round bottomed pressure flask charged with $CsOH\cdot H_2O$ (0.866 g, 5.16 mmol) and a Teflon stir bar, **Ir-Cl** (0.388 g, 0.516 mmol) dissolved in toluene (25 mL) was added. The flask was sealed and heated to 120 °C. After stirring for 24 hours the green-brown solution had turned dark brown-red. This solution was cooled to room temperature and filtered through a pad of Celite® into a 50 mL round bottom flask. All volatiles were removed from the filtrate *in vacuo* and *n*-pentane (20 mL) was vacuum transferred into the flask at −78 °C. The flask was warmed to room temperature and the solution was stirred for 2 hours. All volatiles were removed *in vacuo*. A brown powder (0.301 g, 0.410 mmol) was isolated in 80% yield. Elemental analysis calcd (%): C, 52.37; H, 7.00; N, 3.82. Found (average of 4 trials): C, 53.41; H, 7.25; N, 3.59 (the carbon value is high due to small amounts of unremovable toluene). APCI-MS (M*+) for $C_{32}H_{51}IrN_2OP_2$: calcd: 734.3100. Found: 734.3070. ^{1}H NMR (500 MHz, C_6D_6) δ 6.70 (dvt, $^4J_{HH} = 2.3$ Hz, $J_{HP} = 3.7$ Hz, 2H, ArH), 6.34 (d, $^4J_{HH} = 2.3$ Hz, 2H, ArH), 3.64 (t, $^2J_{HP} = 3.8$ Hz, 1H, **Ir-OH**), 2.95 (m, 4H, $PCH(CH_3)_2$), 2.36 (s, 12H, $N(CH_3)_2$), 1.65 (s, 6H (18H with $PCH(CH_3)_2$), $-C(CH_3)_2-$), 1.63 (dvt, $^3J_{HH} = 7.5$ Hz, $J_{HP} = 7.3$ Hz, 12H (18H with $-C(CH_3)_2-$), $PCH(CH_3)_2$), 1.40 (dvt, $^3J_{HH} = 7.1$ Hz, $J_{HP} = 7.1$ Hz, 12H, $PCH(CH_3)_2$). $^{13}C\{^1H\}$

NMR (126 MHz, C_6D_6) δ 197.0 (t, $^2J_{CP}$ = 2.2 Hz, Ir=C), 158.7 (vt, J_{CP} = 18.8 Hz, ArC), 149.9 (vt, J_{CP} = 3.9 Hz, ArC), 142.5 (vt, J_{CP} = 20.0 Hz, ArC) 130.3 (vt, J_{CP} = 7.8 Hz, ArC), 116.3 (s, ArCH), 114.4 (s, ArCH), 42.7 (s, –$C(CH_3)_2$–), 40.2 (s, $N(CH_3)_2$), 28.2 (s, –$C(CH_3)_2$–), 25.3 (vt, J_{CP} = 12.8 Hz, $PCH(CH_3)_2$), 20.0 (vt, J_{CP} = 2.7 Hz, $PCH(CH_3)_2$), 19.7 (s, $PCH(CH_3)_2$). $^{31}P\{^1H\}$ NMR (203 MHz, C_6D_6) δ 51.9 (s).

Synthesis of Ir-H_4

Method 1: to a 100 mL thick walled glass pressure vessel equipped with a Teflon stirbar, **Ir-OH** (0.196 g, 0.267 mmol) dissolved in benzene (15 mL) was loaded. The mixture was degassed *via* the freeze–pump–thaw method and placed under 4 atm of H_2 gas. After stirring for 3 hours all volatiles were removed *in vacuo* resulting in a dark red-brown residue. To this *n*-pentane (25 mL) were added *via* vacuum transfer at −78 °C. The solution was warmed to room temperature and stirred for 20 minutes under 1 atm of H_2. The *n*-pentane was removed under high vacuum and a beige powder (0.188 g, 0.260 mmol) was isolated in 98% yield. Elemental analysis calcd (%): C, 53.24; H, 7.68; N, 3.88. Found: C, 53.48; H, 8.11; N, 3.73. Method 2: to a 100 mL thick walled glass pressure vessel charged with NaOH (0.266 g, 6.65 mmol) and a Teflon stirbar, **Ir-Cl** (0.500 g, 0.665 mmol) dissolved in benzene (35 mL) was loaded. The mixture was degassed *via* the freeze–pump–thaw method and then placed under 4 atm of H_2 gas. After stirring for 3 hours the now orange-yellow solution was degassed and filtered through a pad of Celite® in a glovebox. The filtrate was placed in a 50 mL round bottom flask and all volatiles were removed *in vacuo*. To the dark-red residue *n*-pentane (25 mL) was vacuum transferred at −78 °C. The mixture was warmed to room temperature, placed under 1 atmosphere of H_2 gas and stirred for 20 minutes. All volatiles were removed *in vacuo* and a beige powder (0.454 g, 0.627 mmol) was isolated in 94% yield. X-ray quality crystals were obtained by slowly cooling a supersaturated solution of **Ir-H_4** in isopropanol from 50 °C to 20 °C. Elemental analysis calcd (%): C, 53.24; H, 7.68; N, 3.88. Found: C, 53.43; H, 7.88; N, 3.80. ^1H NMR (500 MHz, C_6D_{12}) δ 6.84 (d, $^4J_{HH}$ = 1.9 Hz, 2H, ArH), 6.48 (dvt, $^4J_{HH}$ = 1.9 Hz, J_{HP} = 4.0 Hz, 2H, ArH), 5.52 (s, 1H, Ir–CH), 2.85 (s, 12H, $N(CH_3)_2$), 2.10 (m, 2H, $PCH(CH_3)_2$), 1.91 (m, 2H, $PCH(CH_3)_2$), 1.84 (s, 3H, –$C(CH_3)_2$–), 1.23 (s, 3H, –$C(CH_3)_2$), 1.16 (dvt, $^3J_{HH}$ = 7.9 Hz, J_{HP} = 7.4 Hz, 6H, $PCH(CH_3)_2$), 1.07 (m, 12H, $PCH(CH_3)_2$), 0.78 (dvt, $^3J_{HH}$ = 8.0 Hz, J_{HP} = 7.3 Hz, 6H, $PCH(CH_3)_2$), −10.32 (t, $^2J_{HP}$ = 10.7 Hz, 4H). $^{13}C\{^1H\}$ NMR (126 MHz, C_6D_{12}) δ 151.6 (vt, J_{CP} = 15.4 Hz, ArC) 149.2 (vt, J_{CP} = 4.3 Hz, ArC), 145.2 (vt, J_{CP} = 7.4 Hz, ArC) 139.6 (vt, J_{CP} = 24.4 Hz, ArC), 112.1 (s, ArCH), 111.6 (s, ArCH), 41.9 (s, $N(CH_3)_2$), 40.8 (s, –$C(CH_3)_2$–), 30.3 (s, –$C(CH_3)_2$–), 30.1 (vt, J_{CP} = 14.8 Hz, $PCH(CH_3)_2$), 25.0 (s, –$C(CH_3)_2$–), 23.1 (vt, J_{CP} = 16.7 Hz, $PCH(CH_3)_2$), 21.0 (s, Ir–CH), 20.2 (s, $PCH(CH_3)_2$), 20.2 (vt, J_{CP} = 2.2 Hz, $PCH(CH_3)_2$), 19.4 (vt, J_{CP} = 3.7 Hz, $PCH(CH_3)_2$), 18.0 (s, $PCH(CH_3)_2$). $^{31}P\{^1H\}$ NMR (203 MHz, C_6D_{12}) δ 56.5 (s).

Synthesis of Ir-Ph

To a 25 mL round bottom flask equipped with a Teflon stirbar, **Ir-H_4** (0.180 g, 0.249 mmol) dissolved in benzene (10 mL) was added. The solution was stirred at room temperature in a glovebox and *tert*-butylethylene (0.105 g, 1.069 mmol) was added. After stirring for 10 minutes all volatiles were removed *in vacuo*. The dark green-brown residue was then sonicated in *n*-pentane (5 mL). The solid was then filtered through a fritted Büchner funnel and washed with *n*-pentane (3 × 2 mL). A dark green powder (0.143 g, 0.180 mmol) was isolated in 73% yield. X-ray quality crystals were obtained from a saturated solution of **Ir-Ph** in *n*-pentane that was sealed at room temperature in a 20 mL scintillation vial for 1 week. Elemental analysis calcd (%): C, 57.48; H, 6.98; N, 3.53. Found: C, 57.59; H, 6.99; N, 3.52. ^1H NMR (500 MHz, C_6D_6) δ 7.54 (t, $^3J_{HH}$ = 7.4 Hz, 2H, Ph-H), 7.14 (d, $^3J_{HH}$ = 7.3 Hz, 2H, Ph-H), 6.97 (t, $^3J_{HH}$ = 7.3 Hz, 1H, Ph-H), 6.74 (m, 2H, Ar-H), 6.25 (d, $^4J_{HH}$ = 2.2 Hz, 2H, Ar-H), 3.16 (m, 2H, $P(CH(CH_3)_2)$, 2.25 (s, 12H, $N(CH_3)_2$), 1.63 (s, 6H, –$C(CH_3)_2$), 1.40 (dvt, $^3J_{HH}$ = 7.0 Hz, $^3J_{HP}$ = 7.0 Hz 12H, $PCH(CH_3)_2$), 1.35 (dvt, $^3J_{HH}$ = 7.9 Hz, $^3J_{HP}$ = 7.3 Hz 12H, $PCH(CH_3)_2$). $^{13}C\{^1H\}$ NMR (126 MHz, C_6D_6) δ 221.1 (t, $^2J_{CP}$ = 4.0 Hz, C=Ir), 171.8 (vt, J_{CP} = 8.8 Hz, PhC-Ir), 157.7 (vt, J_{CP} = 19.2 Hz, ArC), 151.4 (vt, J_{CP} = 3.9 Hz, ArC), 147.3 (vt, J_{CP} = 17.9 Hz, ArC), 142.2 (vt, J_{CP} = 7.3 Hz, ArC), 140.2 (s, PhCH), 126.6 (s, PhCH), 120.8 (s, PhCH), 116.6 (s, ArCH), 113.7 (s, ArCH), 43.5 (s, –$C(CH_3)_2$–), 40.2 (s, $N(CH_3)_2$), 27.4 (s, –$C(CH_3)_2$–), 24.3 (vt, J_{CP} = 13.3 Hz, $PCH(CH_3)_2$), 20.1 (vt, J_{CP} = 2.4 Hz, $PCH(CH_3)_2$), 19.3 (br s, $PCH(CH_3)_2$). $^{31}P\{^1H\}$ NMR (203 MHz, C_6D_6) δ 53.6 (s).

Generation of Ir-H_3

To a J.-Young tube charged with **Ir-Ph** (0.010 g, 0.025 mmol) dissolved in C_6H_6 (0.25 mL), **Ir-H_4** (0.013 g, 0.037 mmol) in C_6H_6 (0.35 mL) was added dropwise over 5 minutes. The solution changed from dark green to a dark reddish brown color. **Ir-H_3** is generated *in situ* and is unisolable. ^1H NMR (500 MHz, C_6H_6 spiked with C_6D_{12}) δ 6.78 (m, Ar-H), 6.63 (d, $^4J_{HH}$ = 2.5 Hz Ar-H), 2.58 (s, 12H, $N(CH_3)_2$), 2.25 (m, 4H, $PCH(CH_3)_2$), 1.63 (s, 6H, –$C(CH_3)_2$–), 1.46 (dvt, J_{HP} = 7.5 Hz, $PCH(CH_3)_2$), 1.14 (m, $PCH(CH_3)_2$). $^{13}C\{^1H\}$ NMR (126 MHz, C_6H_6 spiked with C_6D_{12}) δ 245.0 (br s, C=Ir); 152.4 (vt, J_{CP} = 19.8 Hz, ArC), 152.1 (vt, J_{CP} = 19.0 Hz, ArC), 150.4 (vt, J_{CP} = 3.3 Hz, ArC), 140.1 (vt, J_{CP} = 6.9 Hz, ArC), 115.4 (s, ArCH), 112.3 (s, ArCH), 41.3 (s, –$C(CH_3)_2$–), 40.8 (s, $N(CH_3)_2$), 32.1 (s, –$C(CH_3)_2$–), 27.3 (vt, J_{CP} = 15.6 Hz, $PCH(CH_3)_2$), 21.9 (s, $PCH(CH_3)_2$), 19.8 (s, $PCH(CH_3)_2$). $^{31}P\{^1H\}$ NMR (203 MHz, C_6D_6) δ 66.4 (s).

Preparation of stock solutions

Solution A: complex **Ir-Ph** (0.060 g, 0.076 mmol, 0.015 M) was dissolved with benzene-d_6 in a volumetric flask (5 mL). *Solution B*: cyclohexane was added to a volumetric flask (5 mL) containing complex **Ir-H_4** (0.068 g, 0.094 mmol, 0.019 M) and cyclohexane-d_{12} (0.550 g, 5.07 mmol, 1.15 M). *Solution C*: cyclohexane was added to a volumetric flask (1 mL) containing *Solution B* (0.450 mL) and substrate (0.85 mmol).

General procedure for deuteration of substrates in C_6D_6

Stock *Solution A* (0.80 mL) was added to a glass reaction tube (length: 8.5 cm length, inner diameter: 1.5 cm) equipped with a Teflon stirbar. The flask was sealed with a rubber stopper and

1.4 mol% (0.405 mL, 0.017 mmol at 20 °C) or 9 mol% (2.6 mL, 0.11 mmol) D_2 gas was injected into the flask. After stirring for 10 minutes at 20 °C, the solution (0.250 mL, 0.0038 mmol of [Ir]) was injected into a J.-Young tube containing substrate (0.38 mmol), cyclohexane (0.046 mmol) and benzene-d_6 (0.75 mL). The solution was heated to 65 °C for 24 hours and conversion was measured using cyclohexane as an internal standard. Cyclohexane was monitored without the use of an internal standard; no detectable traces of deuterium incorporation were visible using ^{1}H, ^{2}H or ^{13}C{^{1}H} NMR.

General procedure for deuteration of substrates in cyclohexane with D_2O

Stock *Solution C* (0.450 mL) was added to a pressure tube (10 mL) charged with cyclohexane (0.300 mL), argon sparged D_2O (0.4 mL, 0.022 mmol) and a Teflon stirbar. Another sample was prepared by placing stock *Solution C* (0.450 mL) and cyclohexane (0.300 mL) in an NMR tube; this sample was used as a starting material reference. The flask was sealed under argon (1 atm) with a Teflon valve and heated to the appropriate temperature. After 24 hours the organic phase was carefully transferred to an NMR tube under argon without exposure to air. Conversion was measured *via* ^{1}H NMR using the cyclohexane signal as the internal standard. The reference samples containing water miscible/soluble compounds (THF, triethylamine, 2, 6-lutidine, pyridine, aniline and phenol) were extracted with D_2O prior to running NMR. The ^{1}H NMR spectra of the organic phases for these samples were compared to the organic phases of the reaction mixtures to measure conversion. Aliquots of the D_2O fractions (0.2 mL) for both the reference and reaction mixtures were also taken and added to separate NMR samples containing D_2O (0.4 mL) and DMSO (10 μL). The ^{1}H NMR spectra for these samples indicated comparable levels of deuteration were present in the D_2O phase.

General procedure for deuteration of neat benzene, fluorobenzene and *n*-heptane with D_2O

Substrate (8.31 mmol) was loaded into a pressure tube (10 mL) charged with **Ir-H$_4$** (0.060 g, 0.083 mmol) and a Teflon stirbar. Argon sparged D_2O (6.0 mL, 330 mmol) was carefully added to the reaction flask under a steady flow of argon. The vessel was sealed with a Teflon valve and heated to 80 °C for 24 hours. The flask containing *n*-heptane was freeze–pump–thawed three-fold and heated to 120 °C under static vacuum for 24 hours. Organic phases were extracted under a flow of argon *via* syringe and liquids were distilled under reduced pressure from the iridium catalyst. Benzene was recovered in 81% yield (0.561 g, 6.72 mmol) with 90% deuterium incorporation. Fluorobenzene was recovered in 82% yield (0.725 g, 6.81 mmol) with 94% deuterium incorporation at all positions. *n*-Heptane was recovered in 88% yield (0.791 g, 7.40 mmol) with 63% deuterium at the terminal methyl positions and 28% deuterium incorporation throughout the methylene position.

Deuteration of THF with D_2O

THF (0.600 g, 8.32 mmol) was added to a pressure tube (10 mL) charged with **Ir-H$_4$** (0.060 g, 0.083 mmol) and a Teflon stirbar. Argon sparged D_2O (6 mL) containing NaOH (1.45 g, 36.3 mmol, 6 M) was added to the flask under a flow of argon. The mixture was freeze–pump–thawed three-fold and sealed under static vacuum. After heating at 100 °C for 24 hours the organic phase was extracted under a flow of argon *via* syringe and distilled under reduced pressure from the iridium catalyst. Deuterated THF was recovered in 84% yield (0.547 g, 7.03 mmol) with deuterium incorporated in 74% and 65% at the 2 and 3 positions, respectively.

Conflicts of interest

There are no conflicts to declare.

Acknowledgements

Funding for this work was provided by NSERC of Canada (Discovery Grant) and the Canada Research Chair secretariat (Tier I CRC 2013–2020) to W. E. P. Author J. D. S thanks NSERC of Canada for PGSD Scholarship support. D. H. E acknowledges the United States National Science Foundation Chemical Structure, Dynamics, and Mechanisms B (CSDM-B) Program for support under award CHE 1952420. We thank Brigham Young University and the Office of Research Computing, especially the Fulton Supercomputing Lab. G. D. thanks the BYU Department of Chemistry and Biochemistry for undergraduate research awards.

Notes and references

1 J. Yang, *Deuterium: Discovery and Applications in Organic Chemistry*, Elsevier, Amsterdam, 2016.
2 J. L. Garnett and R. J. Hodges, *J. Am. Chem. Soc.*, 1967, **89**, 4546–4547.
3 J. L. Garnett and R. S. Kenyon, *J. Chem. Soc. D*, 1971, 1227–1228.
4 N. F. Goldshleger, M. B. Tyabin, A. E. Shilov and A. A. Shteinman, *Zh. Fiz. Khim.*, 1969, **43**, 1222–1223.
5 A. E. Shilov and A. A. Shteinman, *Coord. Chem. Rev.*, 1977, **24**, 97–143.
6 T. G. Gant, *J. Med. Chem.*, 2014, **57**, 3595–3611.
7 R. Pony Yu, D. Hesk, N. Rivera, I. Pelczer and P. J. Chirik, *Nature*, 2016, **529**, 195–199.
8 J. Atzrodt, V. Derdau, W. J. Kerr and M. Reid, *Angew. Chem., Int. Ed. Engl.*, 2018, **57**, 1758–1784.
9 T. Junk and W. J. Catallo, *Chem. Soc. Rev.*, 1997, **26**, 401–406.
10 J. Atzrodt, V. Derdau, T. Fey and J. Zimmermann, *Angew. Chem., Int. Ed. Engl.*, 2007, **46**, 7744–7765.
11 J. Atzrodt, V. Derdau, W. J. Kerr and M. Reid, *Angew. Chem., Int. Ed. Engl.*, 2018, **57**, 3022–3047.
12 R. H. Crabtree, H. Felkin and G. E. Morris, *J. Organomet. Chem.*, 1977, **141**, 205–215.
13 A. H. Janowicz and R. G. Bergman, *J. Am. Chem. Soc.*, 1982, **104**, 352–354.
14 A. H. Janowicz and R. G. Bergman, *J. Am. Chem. Soc.*, 1983, **105**, 3929–3939.

15 B. A. Arndtsen and R. G. Bergman, *Science*, 1995, **270**, 1970–1973.
16 J. T. Golden, R. A. Andersen and R. G. Bergman, *J. Am. Chem. Soc.*, 2001, **123**, 5837–5838.
17 S. R. Klei, J. T. Golden, T. D. Tilley and R. G. Bergman, *J. Am. Chem. Soc.*, 2002, **124**, 2092–2093.
18 G. N. Nilsson and W. J. Kerr, *J. Labelled Compd. Radiopharm.*, 2010, **53**, 662–667.
19 S. R. Klei, T. D. Tilley and R. G. Bergman, *Organometallics*, 2002, **21**, 4905–4911.
20 M. B. Skaddan, C. M. Yung and R. G. Bergman, *Org. Lett.*, 2004, **6**, 11–13.
21 C. M. Yung, M. B. Skaddan and R. G. Bergman, *J. Am. Chem. Soc.*, 2004, **126**, 13033–13043.
22 L. L. Santos, K. Mereiter, M. Paneque, C. Slugovc and E. Carmona, *New J. Chem.*, 2003, **27**, 107–113.
23 J. L. Rhinehart, K. A. Manbeck, S. K. Buzak, G. M. Lippa, W. W. Brennessel, K. I. Goldberg and W. D. Jones, *Organometallics*, 2012, **31**, 1943–1952.
24 S. H. Lee, S. I. Gorelsky and G. I. Nikonov, *Organometallics*, 2013, **32**, 6599–6604.
25 *Topics in Organometallic Chemistry: Organometallic Pincer Chemistry*, ed. G. van Koten and D. Milstein, Springer, Heidelberg, 2013.
26 D. Morales-Morales, *Pincer Compounds: Chemistry and Applications*, Elsevier, Amsterdam, 2018.
27 A. Kumar, T. M. Bhatti and A. S. Goldman, *Chem. Rev.*, 2017, **117**, 12357–12384.
28 N. A. Eberhardt and H. Guan, *Pincer Compounds: Chemistry and Applications*, Elsevier, Amsterdam, 2018.
29 R. Tanaka, M. Yamashita and K. Nozaki, *J. Am. Chem. Soc.*, 2009, **131**, 14168–14169.
30 M. H. G. Prechtl, M. Hoelscher, Y. Ben-David, N. Theyssen, D. Milstein and W. Leitner, *Eur. J. Inorg. Chem.*, 2008, 3493–3500.
31 M. H. G. Prechtl, M. Hölscher, Y. Ben-David, N. Theyssen, R. Loschen, D. Milstein and W. Leitner, *Angew. Chem., Int. Ed. Engl.*, 2007, **119**, 2319–2322.
32 J. Zhou and J. F. Hartwig, *Angew. Chem., Int. Ed. Engl.*, 2008, **47**, 5783–5787.
33 V. M. Iluc, A. Fedorov and R. H. Grubbs, *Organometallics*, 2011, **31**, 39–41.
34 A. V. Polukeev, R. Marcos, M. S. G. Ahlquist and O. F. Wendt, *Organometallics*, 2016, **35**, 2600–2608.
35 R. J. Burford, W. E. Piers and M. Parvez, *Organometallics*, 2012, **31**, 2949–2952.
36 C. C. Comanescu and V. M. Iluc, *Organometallics*, 2014, **33**, 6059–6064.
37 S. Sung and R. D. Young, *Dalton Trans.*, 2017, **46**, 15407–15414.
38 P. Cui and V. M. Iluc, *Chem. Sci.*, 2015, **6**, 7343–7354.
39 S. Sung, Q. Wang, T. Krämer and R. D. Young, *Chem. Sci.*, 2018, **9**, 8234–8241.
40 L. E. Doyle, W. E. Piers and J. Borau-Garcia, *J. Am. Chem. Soc.*, 2015, **137**, 2187–2190.
41 C. Yoo and Y. Lee, *Angew. Chem., Int. Ed.*, 2017, **56**, 9502–9506.
42 D. Sahoo, C. Yoo and Y. Lee, *J. Am. Chem. Soc.*, 2018, **140**, 2179–2185.
43 J. D. Smith, J. R. Logan, L. E. Doyle, R. J. Burford, S. Sugawara, C. Ohnita, Y. Yamamoto, W. E. Piers, D. M. Spasyuk and J. Borau-Garcia, *Dalton Trans.*, 2016, **45**, 12669–12679.
44 J. D. Smith, E. Chih, W. E. Piers and D. M. Spasyuk, *Polyhedron*, 2018, **155**, 281–290.
45 J. D. Smith, J. Borau-Garcia, W. E. Piers and D. Spasyuk, *Can. J. Chem.*, 2016, **94**, 293–296.
46 L. E. Doyle, W. E. Piers, J. Borau-Garcia, M. J. Sgro and D. M. Spasyuk, *Chem. Sci.*, 2016, **7**, 921–931.
47 E. A. LaPierre, W. E. Piers, D. M. Spasyuk and D. W. Bi, *Chem. Commun.*, 2016, **52**, 1361–1364.
48 E. A. LaPierre, W. E. Piers and C. Gendy, *Dalton Trans.*, 2018, **47**, 16789–16797.
49 C. C. Comanescu and V. M. Iluc, *Chem. Commun.*, 2016, **52**, 9048–9051.
50 L. E. Doyle, W. E. Piers and D. W. Bi, *Dalton Trans.*, 2017, **46**, 4346–4354.
51 E. A. LaPierre, W. E. Piers and C. Gendy, *Organometallics*, 2018, **37**, 3394–3398.
52 S. Sung, T. Joachim, T. Krämer and R. D. Young, *Organometallics*, 2017, **36**, 3117–3124.
53 H. Tinnermann, S. Sung, B. A. Cala, H. J. Gill and R. D. Young, *Organometallics*, 2020, **39**, 797–803.
54 R. J. Burford, W. E. Piers, D. H. Ess and M. Parvez, *J. Am. Chem. Soc.*, 2014, **136**, 3256–3263.
55 P. J. Desrosiers, L. Cai, Z. Lin, R. Richards and J. Halpern, *J. Am. Chem. Soc.*, 1991, **113**, 4173–4184.
56 T. J. Hebden, K. I. Goldberg, D. M. Heinekey, X. Zhang, T. J. Emge, A. S. Goldman and K. Krogh-Jespersen, *Inorg. Chem.*, 2010, **49**, 1733–1742.
57 F. Maseras, A. Lledós, M. Costas and J. M. Poblet, *Organometallics*, 1996, **15**, 2947–2953.
58 S. Gründemann, H.-H. Limbach, G. Buntkowsky, S. Sabo-Etienne and B. Chaudret, *J. Phys. Chem. A*, 1999, **103**, 4752–4754.
59 D. Devarajan and D. H. Ess, *Inorg. Chem.*, 2012, **51**, 6367–6375.
60 A. V. Polukeev, R. Marcos, M. S. G. Ahlquist and O. F. Wendt, *Chem. Sci.*, 2015, **6**, 2060–2067.
61 A. V. Polukeev, R. Marcos, M. S. G. Ahlquist and O. F. Wendt, *Chem.–Eur. J.*, 2016, **22**, 4078–4086.
62 R. Corberan, M. Sanau and E. Peris, *J. Am. Chem. Soc.*, 2006, **128**, 3974–3979.
63 Y. Xie, F. Yu, Y. Wang, X. He, S. Zhou and H. Cui, *Fluid Phase Equilib.*, 2019, **493**, 137–143.
64 J. L. Herde, J. C. Lambert, C. V. Senoff and M. A. Cushing, in *Inorganic Syntheses*, ed. G. W. Parshall, John Wiley & Sons, Inc., Hoboken, NJ, USA, 2007, pp. 18–20.
65 G. R. Fulmer, A. J. M. Miller, N. H. Sherden, H. E. Gottlieb, A. Nudelman, B. M. Stoltz, J. E. Bercaw and K. I. Goldberg, *Organometallics*, 2010, **29**, 2176–2179.